Proc. Natl. Acad. Sci. USA
Vol. 85, pp. 6362–6365, September 1988
Biophysics

Comparison of the solution and crystal structures of staphylococcal nuclease with ^{13}C and ^{15}N chemical shifts used as structural fingerprints

HOLLY B. R. COLE, STEVEN W. SPARKS, AND DENNIS A. TORCHIA*

Bone Research Branch, National Institute of Dental Research, National Institutes of Health, Bethesda, MD 20892

Communicated by F. A. Bovey, May 31, 1988

ABSTRACT **We report high-resolution ^{13}C and ^{15}N NMR spectra of crystalline staphylococcal nuclease (Nase) complexed to thymidine 3',5'-diphosphate and Ca^{2+}. High sensitivity and resolution are obtained by applying solid-state NMR techniques—high power proton decoupling and cross-polarization magic angle sample spinning (CPMASS)—to protein samples that have been efficiently synthesized and labeled by an overproducing strain of *Escherichia coli*. A comparison of CPMASS and solution spectra of Nase labeled with either [*methyl*-^{13}C]methionine or [^{15}N]valine shows that the chemical shifts in the crystalline and solution states are virtually identical. This result is strong evidence that the protein conformations in the solution and crystalline states are nearly the same. Because of the close correspondence of the crystal and solution chemical shifts, sequential assignments obtained in solution apply to the crystal spectra. It should therefore be possible to study the molecular structure and dynamics of many sequentially assigned atomic sites in Nase crystals. Similar experiments are applicable to the growing number of proteins that can be obtained from efficient expression systems.**

Chemical shifts of nuclei such as ^{13}C and ^{15}N are sensitive functions of macromolecular conformation. Therefore, comparison of the cross-polarization magic angle sample spinning (CPMASS) spectrum of a crystalline protein with the solution spectrum of the same protein is a direct method of comparing the protein conformations in the two states. With this approach, it has been shown that the crystalline and solution states of myoglobin have the same average conformations in the neighborhoods of the carbon monoxide ligand (1) and the Met-55 and Met-131 sidechains (2). In spite of the promise that these experiments offered for comparing protein crystal and solution structures, other protein crystals have not, to our knowledge, been studied by CPMASS spectroscopy. The major impediment to such studies is the requirement of ≈30 mg of protein samples containing one or perhaps two types of amino acid residues highly enriched with ^{13}C or ^{15}N at specific sites. A second difficulty is making sequence-specific assignments of signals observed in the spectra of the crystalline samples. Recent advances in molecular biology and NMR spectroscopy (3–9) have greatly reduced these difficulties. In addition, CPMASS spectra of protein crystals, in equilibrium with their mother liquor, can now be recorded by using commercially available NMR probes.

Herein we report CPMASS spectra of crystalline staphylococcal nuclease (Nase), complexed with thymidine 3',5'-diphosphate and Ca^{2+}, and labeled with either [*methyl*-^{13}C]methionine or [^{15}N]valine. Because of the high level of label incorporation, the CPMASS spectra have excellent sensitivity and resolution, and chemical shifts observed in the crystals are easily compared with shifts observed in solution. Although previous work has shown that the solution and crystal structures of Nase are similar (10–13), our spectra provide the first comparison of Nase solution and crystal structures using the same measured parameter. In addition, the excellent sensitivity of the CPMASS spectra permits accurate measurements of spinning sideband intensities and relaxation times of single atomic sites in Nase. The analyses of these data will provide information about protein internal motions, spanning a wide range of rates, at assigned sites. Similar studies can be carried out for the growing number of proteins that have been cloned into efficient expression systems.

EXPERIMENTAL PROCEDURES

We have prepared purified Nase, labeled with either [*methyl*-^{13}C]methionine or [^{15}N]valine, from *Escherichia coli* (provided by John Gerlt, University of Maryland) grown in defined medium by procedures similar to those described (5). As a consequence of the construction of the expression vector, the Nase obtained from this system has a heptapeptide leader sequence (Met-Asp-Pro-Thr-Val-Tyr-Ser) appended to the N terminus of the protein. The heptapeptide extension has no effect on enzyme activity or stability (14). Approximately 70 mg of purified Nase was obtained from a 1-liter cell growth that contained either 100 mg of L-[*methyl*-^{13}C]methionine (Merck) or 400 mg of DL-[^{15}N]valine (Merck). In each case, the high-resolution solution state NMR spectrum of Nase showed that the level of incorporation was >80%. Scrambling of the ^{13}C label was undetectable in the solution spectrum, while low level ^{15}N incorporation (≈10%) was observed in ≈10 non-valyl residues in the ^{1}H–^{15}N heteronuclear multiple quantum shift correlation spectrum recorded in solution.

Crystals of the Nase–TDP–Ca^{2+} complex were made by the procedure of Cotton and colleagues (15, 16). We found that small crystals, suitable for spinning experiments, were obtained in a few days with a mother liquor containing 32–36% (wt/wt) 2-methyl 2,4-pentanediol. Before performing CPMASS experiments, Nase crystals were spun in a centrifuge at 25,000 × *g* and 4°C for several days and then examined with an optical microscope. Except for breakage of the larger crystals, which has no effect on the CPMASS spectra, structural deterioration of the sample was not evident.

High-resolution solution state spectra of Nase were recorded on samples having the following composition: H_2O, 90%; $^{2}H_2O$, 10%; NaCl, 100 mM; borate buffer, 50 mM (pH 7.7); Nase, 1.5 mM; TDP, 5 mM; $CaCl_2$, 10 mM. The Nase solutions had pH meter readings in the range 7.4 ± 0.1. ^{13}C spectra were recorded on a homebuilt instrument operating at 6 T, while proton-detected ^{1}H–^{15}N heteronuclear multiple quantum shift correlation spectra were obtained at 12 T on an

The publication costs of this article were defrayed in part by page charge payment. This article must therefore be hereby marked "*advertisement*" in accordance with 18 U.S.C. §1734 solely to indicate this fact.

Abbreviations: CPMASS, cross-polarization magic angle sample spinning; Nase, staphylococcal nuclease; TSP, sodium 3-trimethylsilylpropionate.

*To whom reprint requests should be addressed.

NT 500 spectrometer equipped with a Cryomagnet Systems probe. CPMASS spectra of Nase crystals were recorded on the 6 T instrument with a Doty Scientific probe. Approximately 30 mg of Nase crystals, in equilibrium with their mother liquor, were loaded into 5-mm sapphire rotors. The use of O-ring end caps prevented sample leakage while spinning.

The Nase [*methyl*-^{13}C]methionine chemical shifts measured in solution are relative to sodium 3-[2,2,3,3-$^{2}H_4$]trimethylsilylpropionate (TSP) dissolved in the borate buffer to eliminate susceptibility corrections. The CPMASS spectra are also referenced to the TSP solution, recorded at the magic angle. Although the crystal mother liquor and TSP solutions have different susceptibilities, the susceptibility correction vanishes at the magic angle (17). The Nase [^{15}N]valine chemical shifts measured at 12 T are referenced to liquid ammonia. At 6 T, the ^{15}N shifts of the crystalline and solution samples, each oriented at the magic angle, were measured relative to the same carrier frequency. Both sets of chemical shifts were then referenced to liquid ammonia by using the 12 T solution spectrum. Uncertainties in the solution and crystalline chemical shifts are 0.1 and 0.2 ppm, respectively.

RESULTS

Nase contains five methionine residues, and the high-resolution solution spectrum of Nase labeled with [*methyl*-^{13}C]methionine (Fig. 1*A*) shows peaks at 14.4 and 18.1 ppm due to single methionine methyl carbons and a large peak at 17.1 ppm due to the three remaining methionine methyl carbons. All five methionine methyl signals are resolved in a proton-detected ^{1}H–^{13}C heteronuclear shift correlation spectrum, which shows that the large signal in Fig. 1*A* is due to three methionine methyl carbons having indistinguishable ^{13}C chemical shifts. The large difference in chemical shifts of the signals at 14.4 and 18.1 ppm arises from the different environments in which the two methionine methyl groups reside. The chemical shifts of the three equivalent methyl carbons indicate that the corresponding three methionine side chains are considerably more disordered and flexible than the two methionine residues having resolved signals. This conclusion is supported by the observation that the linewidths of the signals corresponding to the equivalent carbons in the shift correlation spectrum are 2–3 times smaller than the linewidths of signals corresponding to the resolved carbons.

The ^{13}C CPMASS spectrum (Fig. 1*B*) of a suspension of Nase crystals labeled with [*methyl*-^{13}C]methionine is virtually identical to the solution spectrum. The close correspondence of the methionine chemical shifts in the solution and crystal states is strong evidence that the environments of the five methionine methyl carbons are nearly identical in the two phases. This in turn implies that the average protein structure in the neighborhood of the five methionine residues must be essentially the same in solution and in the protein crystals. We note that the linewidths observed in the crystalline state are significantly greater than those observed in solution. This observation could be due to internal motions of the methionine side chain having correlation times in the range of 10^{-3}–10^{-7} s. Such slow motions can broaden the signals observed in CPMASS spectra by a number of well-documented mechanisms (18–20). In contrast, because the overall correlation time of Nase in solution is $\approx 10^{-8}$ s, motions having correlation times in the range of 10^{-3}–10^{-7} s will not affect the ^{13}C linewidth in solution.

Spinning sidebands are not observed in the CPMASS spectrum of Nase labeled with [*methyl*-^{13}C]methionine, even when the spinning rate is reduced to 1 kHz. This result is not surprising, because the chemical shift anisotropy, σ_{33}–σ_{11}, of the methionine methyl carbon is only 30 ppm (21). In contrast, the shift anisotropy of backbone amide ^{15}N nuclei is $\approx$170 ppm (22, 23), and for this reason the CPMASS spectrum of crystalline Nase labeled with [^{15}N]valine (Fig. 2*A*) shows several spinning sidebands in addition to the

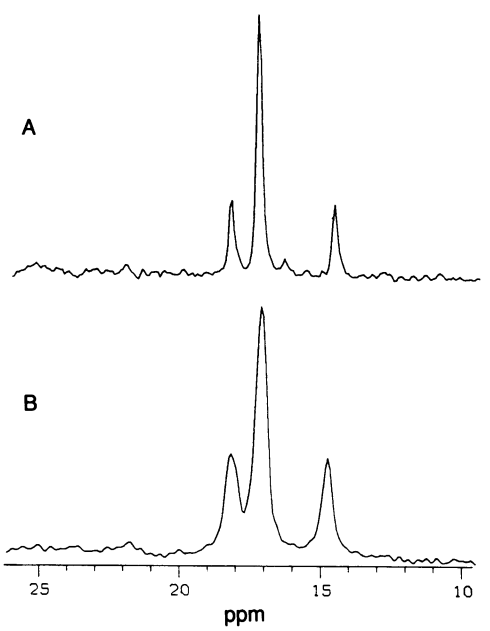

FIG. 1. Comparison of proton-decoupled 62.98 MHz ^{13}C spectra of Nase–TDP–Ca^{2+} labeled with [*methyl*-^{13}C]methionine, 26°C; (*A*) in solution, 90°-t pulse sequence, t = 3 s, 4000 acquisitions; (*B*) crystals, CPMASS spectrum, 2-s recycle delay, 1.3-kHz spinning rate, 1000 acquisitions, ≈50-kHz spin lock and decoupling fields for ^{13}C and ^{1}H, 0.5-ms contact time. Chemical shifts are relative to TSP.

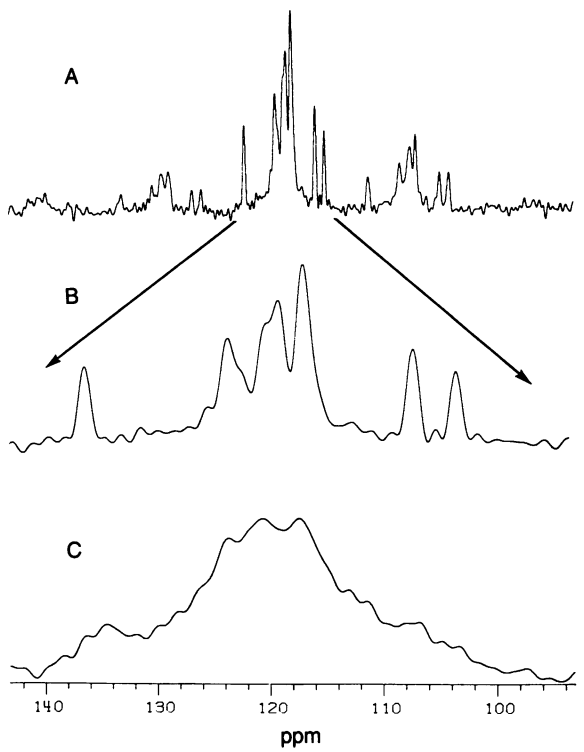

FIG. 2. Proton-decoupled ^{15}N CPMASS spectrum of Nase–TDP–Ca^{2+} complex labeled with [^{15}N]valine at 26°C. (*A*) Center band and spinning sideband spectrum of crystals; (*B*) expanded crystal spectrum showing only the center band; (*C*) center band of spectrum of the lyophilized sample. Recycle delay, 3 s, 15,000 acquisitions, ≈50-kHz spin lock and decoupling fields for ^{15}N and ^{1}H, 0.6-ms contact time. Chemical shifts are relative to external liquid ammonia.

center band. The most interesting feature of this spectrum, seen more clearly in the expanded spectrum of the center band (Fig. 2*B*), is the unusually large dispersion of isotropic chemical shifts (≈33 ppm). This great dispersion in [^{15}N]valine chemical shifts arises from the different structural environments in which the valine residues reside; the chemical shifts are a fingerprint of Nase three-dimensional structure. To quantitate the crystalline chemical shifts, the CPMASS spectrum was simulated (Fig. 3*B*). The chemical shifts, linewidths, and relative intensities that were used to simulate the experimental spectrum are listed in Table 2. The [^{15}N]valine chemical shifts obtained from the proton-detected heteronuclear multiple-quantum shift correlation spectrum of the Nase–TDP–Ca^{2+} complex are listed in Table 1. For purposes of comparison, the solid-state chemical shifts are also listed in Table 1, and the solution chemical shifts are indicated by the vertical lines in Fig. 3*D*.

Examination of the results in Table 1 and Fig. 3 shows that, for 9 of the 10 valine residues in Nase, the chemical shifts derived from the crystal and solution spectra are in close agreement. The single discrepancy involves the 1 valine residue in the heptapeptide extension, which has chemical shifts of 119.7 and 122.0 ppm in the crystalline and solution states, respectively. The signal of the N-terminal valine is readily assigned in solution because it has a large T_2 as a consequence of its high flexibility (T_2 ≡ spin–spin relaxation time). It is therefore likely that the chemical shift of the valine residue in the N terminus is affected by packing of the protein in the crystalline lattice.

The variations in signal intensity shown in Table 2 are a consequence of the short Hartmann–Hahn contact time (0.6 ms) used to obtain the CPMASS spectrum. The use of larger contact times caused a reduction in the signal intensities, a result that indicates that proton rotating frame relaxation times are at most a few milliseconds. Such small relaxation times indicate the presence of slow motions (24), such as

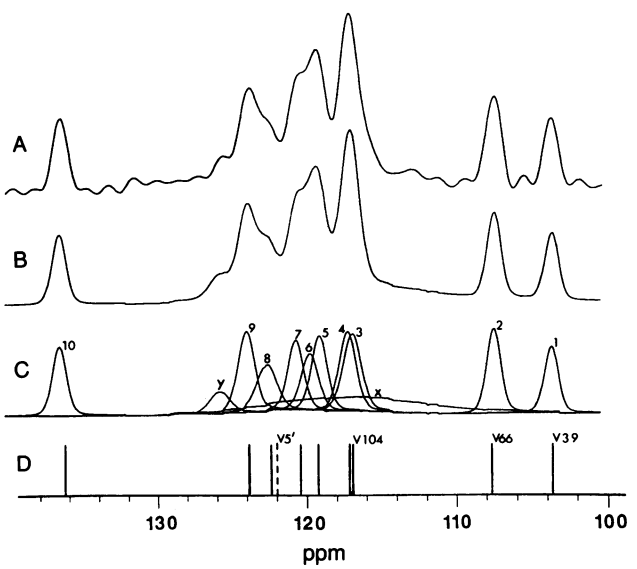

FIG. 3. Comparison of experimental (*A*) and simulated (*B*) proton-decoupled CPMASS center band spectra of the Nase–TDP–Ca^{2+} complex labeled with [^{15}N]valine. The numbered component signals that comprise the simulation (*C*) correspond to the 10 valine residues in Nase, while the signals labeled x and y represent approximately the low level signals due to natural abundance of ^{15}N and to scrambling of the label into other amino acids. The chemical shifts derived from the heteronuclear shift correlation spectrum obtained in solution are indicated by the vertical lines (*D*) and the available sequential assignments are given above the lines. Note that the dashed line is assigned to the valine residue in the heptapeptide extension, and that component line 6 is assigned to this residue in *C*.

Table 1. Comparison of [*methyl*-^{13}C]methionine and [^{15}N]valine chemical shifts of the Nase–TDP–Ca^{2+} complex in the crystalline state and in solution

[*methyl*-^{13}C]-Methionine		[^{15}N]Valine	
Crystals	Solution	Crystals	Solution
14.7	14.4	103.7	103.6
17.1	17.1	107.5	107.7
18.1	18.1	116.9	116.9
		117.2	117.1
		119.1	119.2
		120.6	120.4
		122.6	122.4
		123.9	123.9
		136.5	136.2
		119.7*	122.0*

*Assigned to the valine residue in the N-terminal extension.

those discussed in connection with the [*methyl*-^{13}C]-methionine linewidths.

Fig. 2 affords an interesting comparison of the spectrum of the Nase crystals (Fig. 2*B*) with the corresponding spectrum of the lyophilized protein (Fig. 2*C*). Although there is a rough correspondence of signal intensity in the two spectra, the resolution is clearly far better in the spectrum of the Nase crystals. This result is not surprising, in view of the studies of ^{113}Cd linewidths in cadmium-substituted lyophilized metalloproteins (25, 26). This work indicates that a distribution of protein conformations occurs in the lyophilized state because of nonuniform hydration. A consequence of the distribution of protein conformations is a distribution of isotropic chemical shifts—i.e., linebroadening.

DISCUSSION

Fig. 4 shows that only the N-terminal β-strand and the C-terminal α-helix in Nase lack both valine and methionine residues. Therefore, the close correspondence of the crystal and solution chemical shifts of these residues shows that structure of the Nase–TDP–Ca^{2+} complex must be essentially the same, throughout most of the protein, in the crystalline state and in solution. This result confirms the conclusion of previous less direct comparisons of Nase solution and crystal structures (10–13).

Because isotropic chemical shifts are highly sensitive to protein conformation, the spectra in Figs. 1 and 2 are chemical shift fingerprints that permit one to compare crystal and solution structures. However, it is not yet possible to

Table 2. ^{15}N chemical shifts, linewidths, and integrated signal intensities used to simulate the CPMASS center band spectrum of Nase–TDP–Ca^{2+} crystals labeled with [^{15}N]valine

Line	Chemical shift	Linewidth, Hz	Intensity*
1	103.7	33.6	0.80
2	107.5	34.2	1.05
3	116.9	44.9	1.25
4	117.2	41.2	1.19
5	119.1	38.1	1.03
6	119.7	41.5	0.85
7	120.6	37.5	0.95
8	122.6	48.8	0.82
9	123.9	40.6	1.19
10	136.5	35.1	0.88
x	116.5	366.4	1.81
y	125.7	48.9	0.39

*Average value, for the 10 valine signals, normalized to unity.

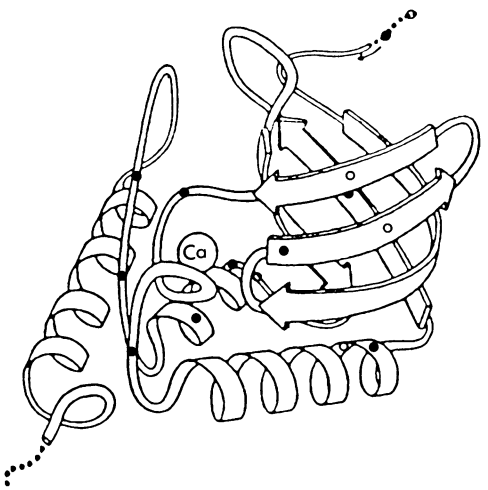

FIG. 4. Diagram of the three-dimensional structure of Nase in the crystalline state, showing the approximate positions of the methionine (○) and valine (●) residues. The drawing of Nase (27) is copyrighted by Jane Richardson and is used with her permission.

correlate a chemical shift measurement with a specific structural feature. To do this, one must first assign the individual signals in the CPMASS spectrum to specific residues in the amino acid sequence. In cases in which solution and solid-state spectra are nearly identical—e.g., Figs. 1 and 3—sequential assignments made in solution (Fig. 3*D*) can be directly carried over to the solid-state spectrum. Alternatively, sequence-specific assignments of backbone atoms can be made directly in the solid state by using the triple resonance techniques developed by Schaefer and colleagues (7, 28). Once assignments are made, the spinning sidebands observed in the CPMASS spectrum (Fig. 2*A*) can be used to determine all three principal elements of the chemical shift tensor of each assigned valine residue (29, 30). One can then compare this large body of chemical shift information with the detailed structural information available from the x-ray data on Nase. Such studies may yield reliable empirical correlations between chemical shift tensor elements and protein structural features.

Magnetization exchange experiments provide information about internuclear distances in solids (31–34), just as in solution (8). The high sensitivity of the CPMASS spectra indicate that such experiments should be straightforward in labeled protein crystals. Indeed, the enhanced sensitivity expected at lower temperatures, where internal motions freeze out, should make two-dimensional spin exchange experiments feasible. Such experiments will be of greatest utility for proteins that form small crystals not suitable for diffraction studies.

Well-resolved CPMASS spectra also provide the opportunity to study protein internal dynamics by analyzing the temperature dependence of linewidths, relaxation times, and sideband intensities. Such studies provide information about slow internal motions that are not usually accessible by solution NMR measurements. In addition, NMR studies of disordered domains in crystals should permit one to ascertain whether the disorder is a consequence of molecular motion.

We thank Prof. John Gerlt for providing us with the transformed *E. coli* used to make Nase, and Rolf Tschudin for expert technical support.

1. Maciel, G. E., Shatlock, M. P., Houtchens, R. A. & Caughey, W. S. (1980) *J. Am. Chem. Soc.* **102,** 6884–6885.
2. Keniry, M. A., Rothgeb, T. M., Smith, R. L., Gutowsky, H. S. & Oldfield, E. (1983) *Biochemistry* **22,** 1917–1926.
3. Shortle, D. (1983) *Gene* **22,** 181–189.
4. Fox, R. O., Evans, P. A. & Dobson, C. M. (1986) *Nature (London)* **320,** 192–194.
5. Hibler, D. W., Stolowich, N. J., Reynolds, M. A., Gerlt, J. A., Wilde, J. A. & Bolton, P. H. (1987) *Biochemistry* **26,** 6278–6286.
6. Oxender, D. L. & Fox, F. C., eds. (1987) *Protein Engineering* (Liss, New York).
7. Schaefer, J., McKay, R. A. & Stejskal, E. O. (1979) *J. Magn. Reson.* **34,** 443–447.
8. Wuethrich, K. (1986) *NMR of Proteins and Nucleic Acids* (Wiley, New York).
9. Griffey, R. H. & Redfield, A. G. (1987) *Q. Rev. Biophys.* **19,** 51–82.
10. Tucker, P. W., Hazen, E. E. & Cotton, F. A. (1978) *Mol. Cell Biol.* **22,** 67–77.
11. Tucker, P. W., Hazen, E. E. & Cotton, F. A. (1979) *Mol. Cell Biol.* **23,** 3–16.
12. Tucker, P. W., Hazen, E. E. & Cotton, F. A. (1979) *Mol. Cell Biol.* **23,** 67–86.
13. Tucker, P. W., Hazen, E. E. & Cotton, F. A. (1979) *Mol. Cell Biol.* **23,** 131–141.
14. Calderon, R. O., Stolowich, N. J., Gerlt, J. A. & Sturtevant, J. M. (1985) *Biochemistry* **24,** 6044–6049.
15. Cotton, F. A., Hazen, E. E., Jr., & Richardson, D. C. (1966) *J. Biol. Chem.* **241,** 4389–4390.
16. Arnone, A., Bier, C. J., Cotton, F. A., Hazen, E. E., Jr., Richardson, D. C. & Richardson, J. S. (1969) *Proc. Natl. Acad. Sci. USA* **64,** 420–427.
17. Earl, W. L. & VanderHart, D. L. (1982) *J. Magn. Reson.* **48,** 35–54.
18. Suwelack, D., Rothwell, W. P. & Waugh, J. S. (1980) *J. Chem. Phys.* **73,** 2559–2569.
19. Rothwell, W. P. & Waugh, J. S. (1981) *J. Chem. Phys.* **74,** 2721–2732.
20. Schmidt, A., Smith, S. O., Raleigh, D. P., Roberts, J. E., Griffin, R. G. & Vega, S. (1986) *J. Chem. Phys.* **85,** 4248–4253.
21. Jelinski, L. W. & Torchia, D. A. (1979) *J. Mol. Biol.* **133,** 45–65.
22. Roberts, J. E., Harbison, G. S., Munowitz, M. G., Herzfeld, J. & Griffin, R. G. (1987) *J. Am. Chem. Soc.* **109,** 4163–4169.
23. Hiyama, Y., Chien-Hua, N., Silverton, J. A., Bavoso, A. & Torchia, D. A. (1988) *J. Am. Chem. Soc.* **110,** 2378–2383.
24. Mehring, M. (1983) *Principles of High Resolution NMR in Solids* (Springer, New York).
25. Marchetti, P. S., Ellis, P. D. & Bryant, R. G. (1985) *J. Am. Chem. Soc.* **107,** 8191–8196.
26. Marchetti, P. S., Bhattacharyya, L., Ellis, P. D. & Brewer, C. F. (1988) *J. Magn. Reson.*, in press.
27. Richardson, J. S. (1981) *Adv. Protein Chem.* **34,** 167–339.
28. Schaefer, J., Stejskal, E. O., Garbow, J. R. & McKay, R. A. (1984) *J. Magn. Reson.* **59,** 150–156.
29. Maricq, M. M. & Waugh, J. S. (1979) *J. Chem. Phys.* **70,** 3300–3316.
30. Herzfeld, J. & Berger, A. E. (1980) *J. Chem. Phys.* **73,** 6021–6030.
31. Caravatti, P., Bodenhausen, G. & Ernst, R. R. (1983) *J. Magn. Reson.* **55,** 88–103.
32. Frey, M. H. & Opella, S. J. (1984) *J. Am. Chem. Soc.* **106,** 4942–4945.
33. Henrichs, P. M., Linder, M. & Hewitt, J. M. (1986) *J. Chem. Phys.* **85,** 7077–7086.
34. VanderHart, D. L. (1987) *J. Magn. Reson.* **72,** 13–47.